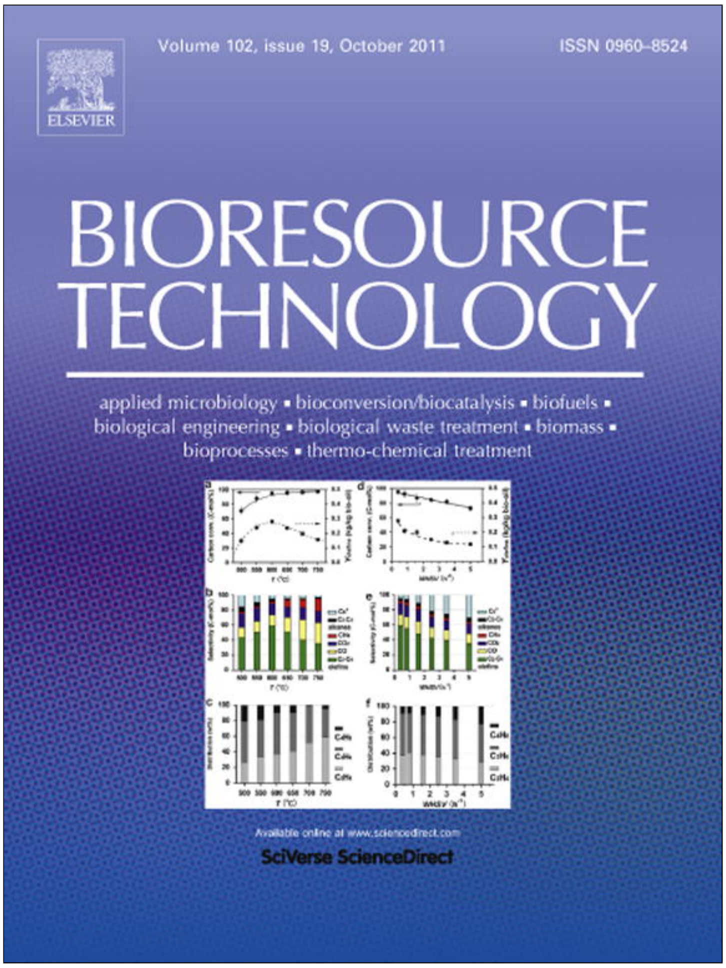

Volume 102, issue 19, October 2011 ISSN 0960-8524

BIORESOURCE
TECHNOLOGY

applied microbiology ▪ bioconversion/biocatalysis ▪ biofuels ▪
biological engineering ▪ biological waste treatment ▪ biomass ▪
bioprocesses ▪ thermo-chemical treatment

Available online at www.sciencedirect.com

SciVerse ScienceDirect

Bioresource Technology 102 (2011) 8877–8884

Contents lists available at ScienceDirect

Bioresource Technology

journal homepage: www.elsevier.com/locate/biortech

Adsorption of copper and zinc by biochars produced from pyrolysis of hardwood and corn straw in aqueous solution

Xincai Chen [a,d], Guangcun Chen [a], Linggui Chen [a], Yingxu Chen [a], Johannes Lehmann [b], Murray B. McBride [b,c], Anthony G. Hay [d,e,*]

[a] Institute of Environmental Science and Technology, Zhejiang University, Hangzhou 310029, PR China
[b] Department of Crop and Soil Sciences, Cornell University, Ithaca, NY 14853, USA
[c] Cornell Center for Waste Management, Cornell University, Ithaca, NY 14853, USA
[d] Department of Microbiology, Cornell University, Ithaca, NY 14853, USA
[e] Institute for Comparative and Environmental Toxicology, Cornell University, Ithaca, NY 14853, USA

ARTICLE INFO

Article history:
Received 3 March 2011
Received in revised form 17 June 2011
Accepted 20 June 2011
Available online 26 June 2011

Keywords:
Biochar
Copper
Zinc
Adsorption kinetic
Adsorption isotherm

ABSTRACT

Biochars produced by pyrolysis of hardwood at 450 °C (HW450) and corn straw at 600 °C (CS600) were characterized and investigated as adsorbents for the removal of Cu(II) and Zn(II) from aqueous solution. The adsorption data were well described by a Langmuir isotherm, with maximum Cu(II) and Zn(II) adsorption capacities of 12.52 and 11.0 mg/g for CS600, 6.79 and 4.54 mg/g for HW450, respectively. Thermodynamic analysis suggested that the adsorption was an endothermic process and did not occur spontaneously. Although Cu(II) adsorption was only marginally affected by Zn(II), Cu(II) competed with Zn(II) for binding sites at Cu(II) and Zn(II) concentrations $\geqslant$1.0 mM. Results from this study indicated that plant-residue or agricultural waste derived biochar can act as effective surface sorbent, but their ability to treat mixed waste streams needs to be carefully evaluated on an individual basis.

1. Introduction

Biochar is a fine-grained and porous substance, similar in appearance to charcoal that is produced by pyrolysis of biomass under oxygen-limited conditions. In recent years, biochar has received considerable interest as a large-scale soil amendment to improve soil fertility, crop production, and nutrient retention and to serve as a recalcitrant carbon stock (Lehmann et al., 2006; Lehmann, 2007a,b; Laird, 2008; Woolf, 2008). Variations in the pyrolysis process greatly affect the qualities of biochar and its potential value to agriculture in terms of agronomic performance or in carbon sequestration. The process and process parameters, principally temperature and furnace residence time, are particularly important; however, the properties of the final product are also dependent upon the nature of the feedstock (Sohi et al., 2009). In general, the carbon content of biochar is inversely related to biochar yield. Increasing pyrolysis temperature from 300 to 800 °C decreased the yield of biochar from 67% to 26% and increased the carbon content from 56% to 93% (Tanaka, 1963). Process temperature also greatly affects the surface area of the biochar. In one study, surface area was shown to increase from 120 m^2/g at 400 °C to 460 m^2/g at 900 °C (Day et al., 2005). These variables together are key influences on the chemical, biological and physical properties, which limit the potential use for biochar products (Sohi et al., 2009).

Biochar has a relatively structured carbon matrix with high degree of porosity and extensive surface area, suggesting that it may act as a surface sorbent which is similar in some aspects to activated carbon and thereby play an important role in controlling contaminants in the environment. Much work has been done on plant-residue or agricultural wastes derived biochar for sorbing organic pollutants (Yang and Sheng, 2003; Chun et al., 2004; Zhu et al., 2005; Wang et al., 2006, 2010; Nguyen et al., 2007; Wang and Xing, 2007; Chen et al., 2008; Chen and Chen, 2009; Yu et al., 2010); however, only limited information is available on metal sorption as well as the associated underlying mechanisms.

While biochars from wood/bark (Mohan et al., 2007), dairy manure (Cao et al., 2009), broiler litter (Uchimiya et al., 2010) and biochars prepared from hydrothermal liquefaction of pinewood and rice husk (Liu and Zhang, 2009) have been shown to sorb significant amounts of heavy metals (such as As, Cd, Pb and Ni), there is very limited research on the effects of different biochars on Cu(II) and Zn(II) adsorption processes. Heavy metal pollutants such as Cu(II) and Zn(II) often coexist in contaminated urban areas, and their mobility is of global concern (Uchimiya et al., 2010). The objective of this study was to investigate the sorption ability of

---

* Corresponding author at: Institute for Comparative and Environmental Toxicology, Cornell University, Ithaca, NY 14853, USA. Tel.: +1 607 255 7571.
E-mail address: agh5@cornell.edu (A.G. Hay).

0960-8524/$ - see front matter © 2011 Elsevier Ltd. All rights reserved.
doi:10.1016/j.biortech.2011.06.078

Cu(II) and Zn(II) by two different biochars derived from hardwood and corn straw in aqueous solution. The mechanisms responsible for contaminant removal were elucidated at different pH, temperature, solid to liquid ratios and using sorption kinetics and isotherms.

2. Methods

2.1. Biochar preparation and characterization

The biochars used in this study were produced by pyrolyzing hardwood and corn straw. One biochar was made from a mix of hardwoods at a temperature of 450 °C with a retention time of less than 5 s (designated as HW450), from Dynamotive Inc., Vancouver, Canada. The other biochar was produced from corn straw under slow pyrolysis conditions at a temperature of 600 °C for 2 h (designated as CS600), from BEST Energies Inc., Madison, Wisconsin, USA. The particle size and size distributions of biochar were measured with a Coulter LS 13 320 (Beckman Coulter, Fullerton, CA, USA). By weight, 3.9% and 12.7% of HW450 and CS600 particles were <0.01 mm, 88.1% and 88.4% were <0.5 mm in diameter, respectively. For HW450, 98% were <1.5 mm, while none of the CS600 particles were >1.5 mm in diameter. Only the fraction that passed through a 0.5 mm sieve was utilized in the experiments described below. The ash content was determined by combusting the biochar at 750 °C for 6 h in open crucibles on a dry weight basis (105 °C for 18 h under argon). The carbon (C), hydrogen (H), and nitrogen (N) contents of all biochars were determined using a CHN elemental analyzer (Flash EA 1112, Thermo Finnigan). The oxygen content was estimated by mass difference (100% – C, H, N and ash %) (Fuertes et al., 2010). Elemental composition was measured in duplicate, and the averaged data are reported. FTIR spectra were collected in the range of 400–4000 cm^{-1} by a Nicolet FTIR spectrophotometer (model 560) with a resolution of 4 cm^{-1}. The specific surface areas (SA) were measured with N_2 adsorption at 77 K determined by a Tristar II3020 surface area analyser (Micromeritics Instrument Co., USA). All samples were outgassed at 105 °C for 16 h before N_2 sorption. The multipoint Brunauer–Emmett–Teller method was employed to calculate surface area, and the meso- and macropore volumes were obtained from desorption isotherms using the Barrett–Joyner–Halenda method (Wang and Xing, 2007). Four data points, with relative pressures of 0.05–0.3, were used to construct the monolayer adsorption capacity. The total pore volume was estimated from a single-N_2 adsorption point at a relative pressure of about 0.97. Biochar pH was measured in a 1:10 suspension of biochar in de-ionized water. The element contents (e.g., K, Ca, Mg, Fe, Mn, Cu and Zn) were analyzed using ICP-OES (IRIS/AP, Thermo Jarrell Ash, USA).

2.2. Metal adsorption experiments

The metal adsorption experiments were performed using a batch equilibration technique. Stock solutions (100 mM) of Cu(II) and Zn(II) were prepared by dissolving analytical grade $Cu(NO_3)_2 \cdot 3H_2O$ and $Zn(NO_3)_2 \cdot 6H_2O$ in distilled water. The kinetic experiments were conducted in 50 ml Erlenmeyer flask by mixing 0.1 g of biochar with 20 ml of 0.01 M $NaNO_3$ solution containing either 1.0 mM Cu(II) or 1.0 mM Zn(II). The mixture was then agitated on a reciprocating shaker at room temperature (22 ± 2 °C) at 120 rpm. Samples were taken at desired intervals and subsequently filtered with Whatman No. 1 filter paper. The filtrates were analyzed for residual heavy metal concentration in the solution. The impact of the solution pH on the metal sorption was investigated in the same way except that the initial pH of the solutions was adjusted to values ranging from 2.0 to 8.0 with the addition of either 0.1 M NaOH or 0.1 M HCl. After 24 h of incubation the metal concentration in filtrates was measured. At the same time, the pH values were also recorded after the biochars-metal suspensions had reached equilibrium. Different amounts of biochar (0.02, 0.1, 0.2, and 1.0 g) were added to 20 ml 0.01 M $NaNO_3$ solution containing 1.0 mM Cu(II) or Zn(II) and the adsorption efficiency and total removal were determined. Adsorption isotherms were obtained at constant pH 5 and 0.01 M ionic strength. During these experiments the initial Cu(II) and Zn(II) concentrations varied from 0.1 to 5.0 mM. The samples were handled in the same manner as described above for the pH experiments. To evaluate and compare the adsorption capacities of Cu(II) and Zn(II) by HW450 and CS600, Langmuir and Freundlich models were used to fit the experimental data. The equations of the Freundlich and Langmuir adsorption models are expressed, respectively, by

$$q_e = \frac{Q_{max} b C_e}{1 + b C_e} \tag{1}$$

$$q_e = K_f C_e^{1/n} \tag{2}$$

where q_e is the amount of the metal adsorbed per unit weight of biochar (mg/g), C_e is the equilibrium concentration of solution (mg/L), Q_{max} is the maximum adsorption capacity (mg/g) and b the constant related to the affinity. K_f and n are indicators of adsorption capacity and intensity, respectively. Q_{max} and b can be determined from the linear plot of C_e/q_e versus C_e. The values of K_f and n were evaluated from the intercept and the slope, respectively, of the linear plot of $\ln q_e$ versus $\ln C_e$ based on the experimental data.

The temperature effect was assessed by equilibrating 0.1 g biochar with 20 ml 0.01 M $NaNO_3$ solution containing 1.0 mM of either Cu(II) or Zn(II) on shaker at 22, 30 and 37 °C. The thermodynamics of the adsorption processes were estimated using the following equations:

$$K_e = \frac{q_e}{C_e} \tag{3}$$

$$\Delta G^o = -RT \ln K_e \tag{4}$$

$$\Delta G^o = \Delta H^o - T\Delta S^o \tag{5}$$

$$\ln K_e = \frac{\Delta S^o}{R} - \frac{\Delta H^o}{RT} \tag{6}$$

where q_e (mg/g) is the amount of heavy metals adsorbed onto the biochars from the solution at equilibrium, C_e (mg/L) the equilibrium concentration of heavy metals in the solution, R (J/mol·K) the gas constant 8.314, T (K) the absolute temperature, and K_e (L/g) the adsorption equilibrium constant. By plotting $\ln K_e$ against $1/T$, the values of $\Delta H^o$and ΔS^ocan be estimated from the slopes and intercepts and the values of ΔG^ocan be obtained from the corresponding values of ΔH^o and ΔS^o.

In order to determine the competitive adsorption characteristics of copper and zinc in a binary-solute system, the initial concentrations of both Cu(II) and Zn(II) were 0.1, 1.0 and 2.0 mM, respectively. Concomitantly, the individual metals (0.1, 0.2, 1.0, 2.0, and 4.0 mM) were also evaluated.

The concentrations of initial and final Cu(II) and Zn(II) in the adsorption experiments were determined using atomic absorption spectrometry (AAS, Buck Scientific Model 200). All experiments were conducted in duplicate. Control experiments without biochar were carried out in order to determine the degree of removal of Cu(II) and Zn(II) from solution by the Erlenmeyer flask. Extraneous metal contamination was found to be negligible.

3. Results and discussion

3.1. Characterization of the biochars

The physico-chemical characteristics of the two different biochars used in this experiment are shown in Table 1. It was found that HW450 was weakly acidic, while the pH of CS600 rose to 9.54. Abe et al. (1998) indicated that cellulose and hemicelluloses could be decomposed around 200–300 °C, producing organic acids and phenolic substances that lowered the pH of the products. Beyond 300 °C, alkali salts begin to separate from the organic matrix and increase the pH of the product. After all the alkali salts are released from the pyrolytic structure, the pH becomes constant at a temperature around 600 °C (Shinogi and Kanri, 2003). The higher pH of CS600 suggests that it has potential as an amendment to neutralize soil acidity, which can be an important factor in metal mobility (Dudka and Adriano, 1997). The ash content of CS600 (60.19%) was higher than that of HW450 (38.55%), which is consistent with the ash content of similar feedstocks (Sassner et al. 2008).

HW450 contained higher concentrations of C and H than CS600. This was likely the result of differences in both the feedstocks and pyrolysis conditions: Demirbas (1997) and Fuertes et al. (2010) found that the C content was higher in hardwood than corn stover, while Chun et al. (2004) and Chen et al. (2008) demonstrated that the C content increased with increasing pyrolysis temperature. The degree of carbonization may be described by the molar H/C ratio, because H is primarily associated with plant organic matter (Kuhlbusch, 1995). In comparison with activated carbon (AC) with H/C ratios of 0.12 (Chun et al., 2004) and 0.256 (Chen et al., 2008), the observed H/C ratios of 0.52 and 0.55 for HW450 and CS600, respectively, indicate that these biochars are weakly carbonized and are consistent with only moderate amounts of aromatization (Chun et al., 2004). These high H/C ratios suggest that both biochars likely still contain a certain amount of original plant organic residues such as cellulose (Chun et al., 2004). The molar oxygen to carbon (O/C) ratio of biochar has been used as a surrogate for surface hydrophilicity since it is indicative of polar-group content, derived most likely from carbohydrates (Chun et al., 2004). Based on that assumption, HW450 is likely to be more hydrophilic than CS600, as it has a higher O/C ratio (0.08 vs 0.04).

CS600 was abundant in mineral elements, especially K and Al (208 and 245 mg/kg, respectively); however, the concentrations of Cu and Zn in both biochars were extremely low (0.11 and 0.67 mg/kg for HW450, 0.18 and 0.95 mg/kg for CS600, respectively) and thus negligible with respect to the adsorption experiments.

The specific surface areas (SA) and total pore volumes (TPV) of CS600 (SA = 13.08 m^2/g and TPV = 0.014) were much higher than those of HW450 (SA = 0.43 m^2/g and TPV = 0.00036). The SA for CS600 was similar to that of a biochar produced from corn stover (SA = 17.3 m^2/g) by Spokas and Reicosky (2009), but significantly lower than a pine needle-derived biochar produced at 600 °C (SA = 206.7 m^2/g and TPV = 0.0764) (Chen et al., 2008). The differences between CS600 and HW450 are consistent with previous reports which found that the surface area of biochar increased with increasing pyrolysis temperatures (Chun et al., 2004; Chen et al., 2008; Cao and Harris, 2010). Comparison of the SA numbers for the biochars used in the present study with reports of other biochars produced at the same temperature suggests that the parent biomass composition, rather than biochar production procedure, played a major role in the SA of biochar. Given the importance of surface area on adsorption, especially for organic molecules (Shinogi and Kanri, 2003), surface area might have some impact on the adsorption of heavy metals.

Surface area also gives an indication of the extent of porosity as highly porous structures, especially microporous structures, have high a surface area (Shinogi and Kanri, 2003). SEM images of HW450 and CS600 (Supplemental Fig. S-1) revealed that CS600 had more pores, which is consistent with its higher BET surface area. The biochar structures were not homogeneous and irregular pores with different shapes and sizes were observed. Given the differences in SA and porosity, it was not surprising that the adsorption capacity of CS600 was larger for heavy metals than that of HW450 in the adsorption experiments.

The FTIR spectra (Supplemental Fig. S-2) of biochars revealed a broad band near 3400 cm^{-1} arising from the stretching vibration of hydroxyl groups and indicated significant hydrogen-bonding interactions. The bands at 2940 and 2904 cm^{-1} were assigned to the $-CH_2$ and $-CH_3$ groups, respectively, of long-chain aliphatic components (Das et al., 2009). The unresolved shoulder near 1730 cm^{-1} and the band at 1650 cm^{-1} were assigned to the stretching vibration of ester carbonyl groups and C = O stretching vibrations of amides, respectively (Das et al., 2009). These latter bands were observed only in HW450. The presence of COO– groups are consistent with the peak at approximately 1570 cm^{-1} which is typically attributed to antisymmetric stretching vibration (Behr et al., 1998), and was observed in both HW450 and CS600. Bands at 1373 and 1443 cm^{-1} were assigned to $-CH_2-$ scissoring. The band at 1262 cm^{-1} was assigned to aromatic CO– and phenolic –OH stretching (Chun et al., 2004) and was observed only in HW450. In CS600, the band indicative of aliphatic ethers (C–O–C) and alcohols –OH (1160–1030 cm^{-1}) is consistent with the oxygenated functional groups of cellulose (Bustin and Guo, 1999), which would be found in the original feedstock. A minor band at 876 cm^{-1} was assigned to the γ–CH of furan; the band at 781 cm^{-1} was assigned to the β–rings of pyridines (Das et al., 2009). Overall, the FTIR results demonstrate qualitative differences in the surface functional groups of the two biochars that were likely due to differences in both the original feedstocks as well as differences in the pyrolysis conditions. The type and concentration of surface functional groups has been reported to play an important role in the adsorption capacity and the removal mechanism of the adsorbates (Yenisoy-Karakas et al., 2004). Even though HW450 contained a larger number of oxygen-containing functional groups, and a higher O/

Table 1
Physico-chemical characteristics of the two different biochars[a].

Properties of biochar	HW450	CS600
pH	5.57	9.54
Moisture content (%)	4.39	4.76
Ash content (%)	38.55	60.19
C (%)	53.41	35.88
H (%)	2.30	1.64
N (%)	0.07	0.43
O (%)	5.67	1.86
(O + N)/C	0.08	0.05
O/C	0.08	0.04
H/C	0.52	0.55
SA (m^2/g)	0.43	13.08
TPV (cm^3/g)	0.00036	0.014
K (mg/kg)	32.95	208.47
Ca (mg/kg)	27.22	27.34
Mg (mg/kg)	4.42	26.37
Na (mg/kg)	5.55	20.08
Fe (mg/kg)	9.33	72.76
Al (mg/kg)	19.44	245.17
P (mg/kg)	0.59	2.51
Mn (mg/kg)	0.98	1.84
Cu (mg/kg)	0.11	0.18
Zn (mg/kg)	0.67	0.95

[a] H/C: atomic ratio of hydrogen to carbon. O/C: atomic ratio of oxygen to carbon. (O + N)/C: atomic ratio of sum of nitrogen and oxygen to carbon. SA: BET-N_2 specific surface area. TPV: total pore volume.

C ratio (Table 1), it had a lower adsorption capacity for heavy metals. This suggests that SA may therefore be more important than the presence of specific functional groups when it comes to metal binding.

3.2. Effect of solution pH

The pH significantly affected the adsorption of Cu(II) and Zn(II) adsorption onto the biochars and was more pronounced for CS600 than HW450 (Fig. 1A). The adsorption capacity increased with increasing pH until it plateaued at pH 5. Others have also made similar observations regarding the adsorption of other metals onto biochar. For example, biochars prepared from hydrothermal liquefaction of pinewood and rice husk achieved their maximum lead removal capacities at pH 5.0 (Liu and Zhang, 2009). Mohan et al. (2007) found the maximum adsorption occurred over a pH range of 3∼4 for arsenic and 4∼5 for lead and cadmium by chars produced from fast pyrolysis of wood and bark. These results can be explained by competition between protons and metal cations for surface sorption sites on the biochars (Martinsa et al., 2004). While at pHs higher than five, the decreasing trend was likely caused by the formation of hydroxide complexes.

Measurements of the change in solution pH after biochar addition and adsorption equilibrium showed that both biochars had a buffering capacity that was distinct from that of the electrolyte (Fig. 1B). This buffering capacity increased the pH of biochar/solution mixtures when the original solution pH was below five, and in general, decreased the pH of mixtures when the original solution pH was above five. For this reason, the speciation of heavy metals in the solution after biochar addition was calculated assuming an initial pH of five with MINTEQA2 model. Under these conditions the model predicted that most of the copper and zinc were present in their free ionic forms (Cu^{2+} and Zn^{2+}). Therefore, all the other experiments in this study were carried out at optimum initial pH of five so as to achieve maximum heavy metal adsorption capacity.

3.3. Adsorption kinetics

Fig. 2 presents the effect of contact time on Cu(II) and Zn(II) adsorption onto biochars. The rate of heavy metal adsorption was fast, with 77–83% of the ultimate adsorption occurring in the first 120 min, followed by a very slow approach to equilibrium. Liu and Zhang (2009) showed the contact time for 95% of the lead removal equilibrium was less than 5 h in the concentration range of 10–20 mg/L. Mohan et al. (2007) also found that 40–70% of the total lead adsorption occurred within the first hour. Generally, sorption seemed to approach equilibrium within 24 h, so the shaking time was fixed for 24 h for all batch experiments. Pseudo-first-order (Eq. (7)) and pseudo-second-order (Eq. (8)) kinetic models were fit to the experimental data to elucidate the heavy metal adsorption mechanism onto the biochars.

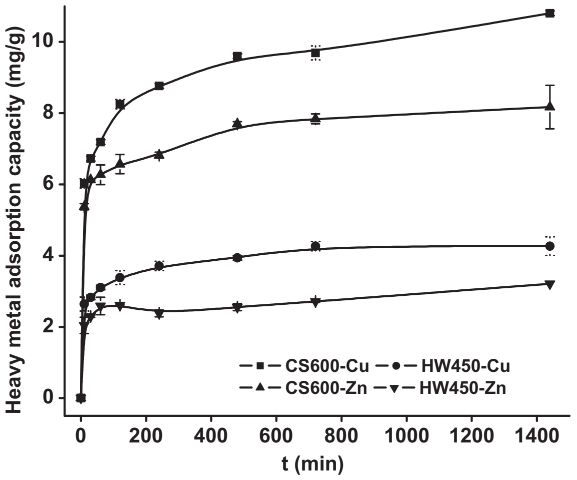

Fig. 2. Effect of contact time on copper and zinc adsorption capacities by CS600 and HW450.

$$\log(q_e - q_t) = \log q_e - \frac{k_1 t}{2.303} \tag{7}$$

$$\frac{t}{q_t} = \frac{1}{k_2 q_e^2} + \frac{t}{q_e} \tag{8}$$

where q_t and q_e (mg/g) are adsorbed heavy metal amount at time t (h) and equilibrium, k_1 (1/h) and k_2 (g/(mg·h)) are the rate constants for the pseudo-first-order and pseudo-second-order adsorption kinetics, respectively.

The plot of $\log(q_e - q_t)$ vs. t should give a linear relationship from which k_1 and q_e can be determined from the slope and the intercept of the plot, respectively. The linear plots of t/q_t against time t can give the pseudo-second-order adsorption rate constant k_2 from the slope and q_e can be calculated from the intercept. The values k_1 and k_2, calculated q_e values and the correlation coefficients R^2 are presented in Table 2. As can be seen from the results,

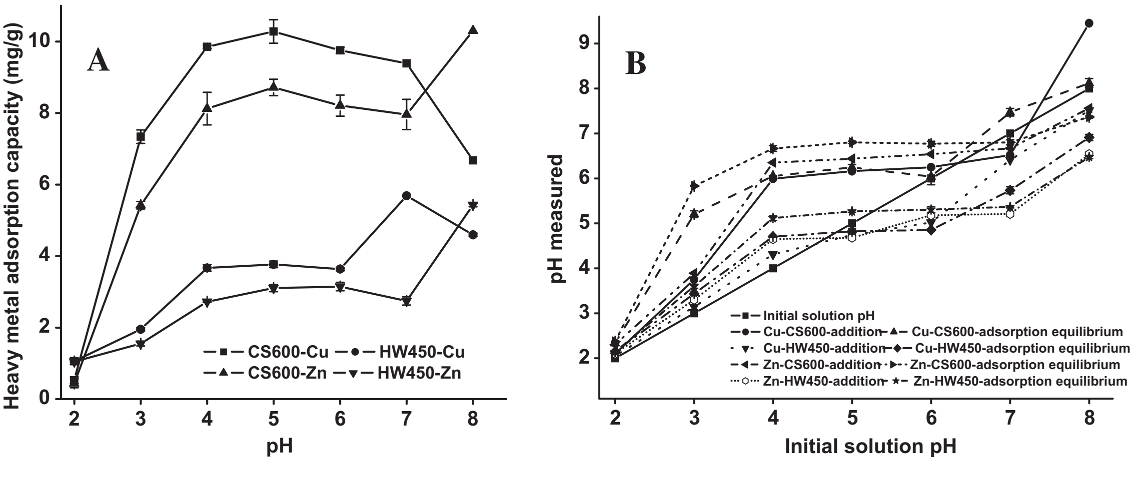

Fig. 1. Effect of initial solution pH on copper and zinc adsorption capacities by CS600 and HW450 (A) and the pH changes of solution after biochar addition and adsorption equilibrium (B) (adsorbent dose 5 g/L; initial heavy metal concentration 1 mM).

Table 2
Parameters of pseudo-first-order and pseudo-second-order kinetics models for copper and zinc onto CS600 and HW450.

Biochar	Heavy metal	Pseudo-first-order model			Pseudo-second-order model		
		q_e	k_1	R^2	q_e	k_2	R^2
CS600	Cu	8.93	0.083	0.865	10.76	0.003	0.996
	Zn	7.11	0.130	0.921	8.20	0.006	0.999
HW450	Cu	3.70	0.100	0.876	4.31	0.011	0.999
	Zn	2.63	0.141	0.923	3.14	0.009	0.988

the correlation coefficients were highest ($R^2 > 0.988$) for the pseudo-second-order model which suggests that that it can be applied for the entire adsorption process. It was also confirmed by the observation that chemisorption was the rate-limiting mechanism for the adsorption of Cu(II) and Zn(II) onto biochars. From these adsorption rate constants, it appears that both Cu(II) and Zn(II) adsorbed more quickly to HW450 than CS600, even though the total sorbed by HW450 was less.

3.4. Effect of adsorbent concentration

The highest observed metal sorption efficiencies for both CS600 and HW450 were at 1 g of biochar/L. For Cu(II) these were 11.8 and 3.71 mg/g, respectively, while for Zn(II) they were 7.48 and 4.98 mg/g, respectively (Fig. 3A). For Cu(II), these are of a similar magnitude, albeit somewhat lower than those reported previously (Samonin et al., 2008; El-Sofany et al., 2009). Increasing the concentration of biochar, however, actually decreased the adsorption efficiency of both CS600 and HW450 (Fig. 3A). For example, the Cu(II) adsorption efficiency of CS600 sharply decreased from 11.82 mg/g at 1 g/L to 1.18 mg/g at 50 g/L. This was likely due to aggregation which was clearly visible at higher biochar concentrations. Despite this decrease in removal efficiency, increasing the adsorbent concentration did result in an increased percentage of the total heavy metals removed (Fig. 3B). For example, while at 1 g biochar/L, the removal of Cu(II) was 6.2% (HW450) and 19.7% (CS600), at 50 g biochar/L it was 56.7% (HW450) and 98.3% (CS600). It should be noted that for CS600 there was no significant difference in the percentage of total Cu(II) or Zn(II) removed by the 10 g biochar/L and 50 g biochar/L concentration, both of which resulted in 95% Cu(II) and 90% Zn(II) removal, whereas the differences in total metal removal for HW450 were significantly different at 10 g biochar/L and 50 g biochar/L ($P < 0.01$). While the observed trend of increased metal removal with increased adsorbent concentration (Fig. 3B) was likely simply a function of the increase in total amount of active sites (Bhattacharyaa et al., 2006), the data suggest that not all of the added sites were available for binding, which is consistent with the observed aggregation.

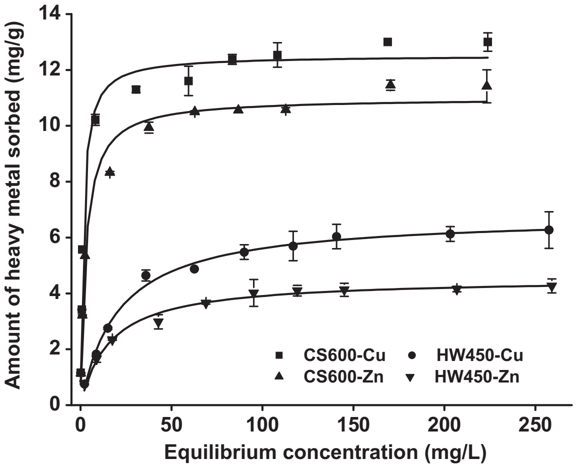

Fig. 4. Sorption isotherms of copper and zinc by CS600 and HW450 in aqueous solution.

3.5. Adsorption isotherms

The Cu(II) and Zn(II) adsorption isotherms were studied at different initial heavy metal concentrations ranging from 0.1 to 5.0 mM and are shown in Fig. 4. The adsorption constants and correlation coefficients for Cu(II) and Zn(II) onto CS600 and HW450 obtained from Langmuir and Freundlich isotherms are given in Table 3. Correlation coefficients suggested that the Langmuir model fit the data better than the Freundlich model ($R^2 > 0.998$ for Langmuir model vs 0.86–0.94 for Freudlich model).

The maximum adsorption capacities of CS600 for Cu(II) and Zn(II) (12.52 and 11.0 mg/g, respectively) were higher than those of HW450 (6.79 and 4.54 mg/g, respectively). The parameter *b* is related to the affinity of the binding sites, which allows comparisons of the affinity of biochar towards the metal ions. CS600 had a higher affinity for Cu(II) and Zn(II) (0.682 and 0.232 L/mg, respectively) than did HW450 (0.048 and 0.061 L/mg, respectively).

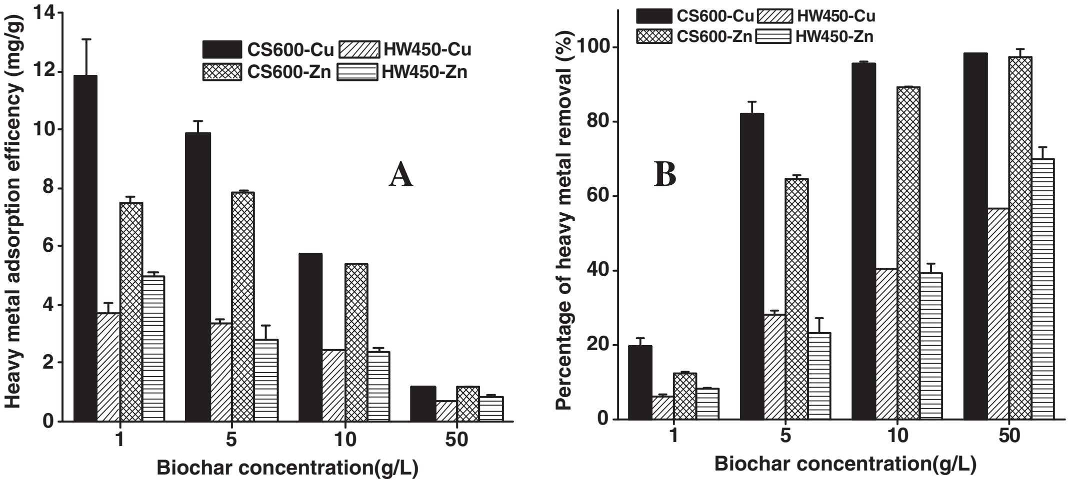

Fig. 3. Effect of biochar concentration on copper and zinc adsorption efficiencies and the percentages of heavy metal removal by CS600 and HW450.

Table 3
Constants and correlation coefficients of Langmuir and Freundlich models for copper and zinc adsorption onto CS600 and HW450 (adsorbent dose 5 g/L).

Biochar	Heavy metal	Langmuir model			Freundlich model		
		Q_{max}	b	R^2	K_f	n	R^2
CS600	Cu	12.52	0.682	0.999	3.71	3.605	0.860
	Zn	11.00	0.232	0.998	2.84	3.336	0.898
HW450	Cu	6.79	0.048	0.999	0.71	2.294	0.928
	Zn	4.54	0.061	0.998	0.72	2.827	0.941

Table 4
Thermodynamic parameters of copper and zinc adsorption onto CS600 and HW450.

Biochar	Heavy metal	Temperature T (K)	Thermodynamic parameters		
			ΔG^o (kJ/mol)	ΔH^o (kJ/mol)	ΔS^o (J/mol K)
CS600	Cu	295	−0.80	25.27	88.21
		303	−1.39		
		310	−2.13		
	Zn	295	1.45	30.94	99.85
		303	0.68		
		310	−0.05		
HW450	Cu	295	5.38	9.22	13.09
		303	5.20		
		310	5.19		
	Zn	295	6.39	7.55	3.99
		303	6.31		
		310	6.34		

Because of variation in parameters and experimental conditions used, direct comparison with other published results should be regarded as tentative, however, the adsorption capacities of CS600 and HW450 exceeded or were comparable to biochar from non-activated date-pits (9.52 and 5.88 mg/g for Cu(II) and Zn(II), respectively) (Banat et al., 2002), shells of lentil, wheat and rice (8.98, 7.39 and 1.85 mg/g for Cu(II), respectively) (Aydin et al., 2008) and modified activated carbon (9.9 mg/g for Zn(II)) (Monser and Adhoum, 2002).

3.6. Thermodynamic studies

The thermodynamic parameters, the values of enthalpy ΔH^o, and entropy ΔS^o, and Gibbs free energy ΔG^o of sorption are useful in defining whether sorption is endothermic or exothermic. Adsorption studies were carried out at three temperatures 22, 30 and 37 °C and the results are shown in Fig. 5. Higher temperatures favored a slight, but statistically significant increase in Cu(II) and Zn(II) adsorption onto CS600 and HW450 ($P < 0.01$), indicating that adsorption was an endothermic process. For example, the Zn(II) adsorption capacity of CS600 increased from 8.65 mg/g at 22 °C to 9.84 mg/g at 37 °C. These results were consistent with a previous report that Pb(II) uptake increased with an increase in temperature for oak wood char and oak bark char in the range of 5–40 °C (Mohan et al., 2007) and with the work of Liu and Zhang (2009), who suggested that increased temperatures provided heavy metals ions sufficient energy to overcome the diffuse double layer and adsorb onto biochar's interior structure (Liu and Zhang, 2009).

The thermodynamic parameters of Cu(II) and Zn(II) adsorption onto CS600 and HW450 are shown in Table 4. The decreasing (increasingly negative) Gibbs free energy values with increasing temperature for the sorption of Cu(II) onto CS600 indicate that it was the most favorable reaction of those tested with these biochar/metal combinations. Although the Gibbs free energy of Zn(II) adsorption onto CS600 also decreased with increasing temperature, it was only negative at 37 °C, which suggests the adsorption might not occur spontaneously. These results contrast with those obtained for HW450 which showed no obvious trend in Gibbs free energy with increasing temperature. Overall, however, the relative trend in ΔG^o values obtained in this study were consistent with the observed trend in metal adsorption capacity (CS600 was lower than HW450), even though it is unclear what is driving the adsorption of either Cu(II) or Zn(II) onto HW450 since those ΔG^o values were positive at all of the temperatures tested. This contrasts somewhat with the work of Liu and Zhang (2009) showed that Gibbs free energy during lead adsorption by a pinewood and rice husk biochar was negative for all test temperatures.

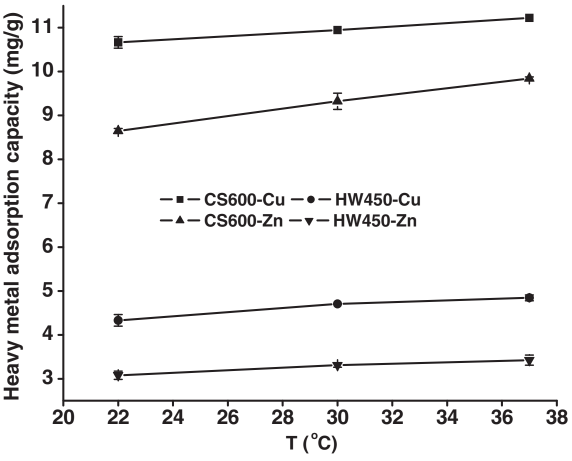

Fig. 5. Effect of temperature on copper and zinc adsorption capacities by CS600 and HW450.

3.7. Adsorption of Cu(II) and Zn(II) in a binary-solution system

In natural environments, heavy metals rarely occur alone and their associations and interactions with one another and with other matrix components are known to influence their transport and fate in the environment (Mingorance and Oliva, 2006). Since Cu(II) and Zn(II) often coexist in contaminated urban sites, their competitive adsorption characteristics in single and binary-solute systems were investigated with the results shown in Table 5. The data clearly show that adsorption of either copper or zinc onto CS600 and HW450 was only minimally affected by the presence of the other metal in solutions at low initial heavy metal concentrations (0.1 mM Cu(II) or Zn(II)). These results suggest that at low concentrations Cu(II) and Zn(II) either bind to different sites on the surface of biochars or that there are excess binding sites so that very little competition occurs. Even at higher concentrations, Zn(II) additions had very little affect on Cu(II) adsorption for either HW450 or CS600 (Cu(II) adsorption, with changes less than 20% on average in the presence of equimolar Zn(II)). However, those results contrast dramatically with the impact of higher Cu(II) concentrations on Zn(II) adsorption: the Zn(II) adsorption capacity of CS600 and HW450 decreased by approximately 75–85% in the presence of Cu(II) concentrations >1 mM, even though the total heavy metal adsorption capacity of CS600 and HW450 in the binary system was similar to that obtained for the individual metals. These results clearly suggest that Cu(II) can compete with Zn(II)-binding sites at higher heavy metal concentrations. This competition is likely due to the higher affinity of the biochars for Cu(II) than Zn(II), which is consistent with the results of the adsorption isotherm experiments (Fig. 4). Seco et al. (1997) also found that Cu(II) removal by activated carbon was not appreciably affected by the presence of Zn ions and Zn(II) adsorption only decreased by 10% as the Cu(II) concentration increased. This comparison suggests that there may be important differences between activated

Table 5
Sorption of copper and zinc from single and binary metal solutions by CS600 and HW450.

Heavy metal concentration	Heavy metal sorption capacity (mg/g)					
	Cu		Zn		Cu + Zn	
	CS600	HW450	CS600	HW450	CS600	HW450
0.1 mM Cu or Zn	1.20 ± 0.01	0.73 ± 0.01	1.13 ± 0.01	0.75 ± 0.01	–	–
0.2 mM Cu or Zn	2.36 ± 0.02	1.23 ± 0.01	2.23 ± 0.01	1.26 ± 0.01	–	–
0.1 mM Cu + 0.1 mM Zn	1.13 ± 0.03	0.64 ± 0.01	1.08 ± 0.01	0.61 ± 0.01	2.22 ± 0.03	1.25 ± 0.01
1.0 mM Cu or Zn	10.57 ± 0.26	4.33 ± 0.13	8.43 ± 0.21	3.08 ± 0.09	–	–
2.0 mM Cu or Zn	12.20 ± 0.01	5.31 ± 0.01	10.40 ± 0.25	4.01 ± 0.05	–	–
1.0 mM Cu + 1.0 mM Zn	9.27 ± 0.13	3.77 ± 0.13	2.10 ± 0.02	0.78 ± 0.03	11.37 ± 0.16	4.56 ± 0.10
2.0 mM Cu or Zn	12.20 ± 0.01	5.31 ± 0.01	10.40 ± 0.25	4.01 ± 0.05	–	–
4.0 mM Cu or Zn	14.34 ± 0.01	6.71 ± 0.26	12.20 ± 1.12	4.65 ± 0.20	–	–
2.0 mM Cu + 2.0 mM Zn	11.83 ± 0.26	5.59 ± 0.13	1.57 ± 0.10	0.96 ± 0.26	13.40 ± 0.16	6.55 ± 0.39

carbon and biochar that need to be taken into account before they can be relied upon for treating mixed waste streams.

4. Conclusions

This study investigated the ability of two different biochars derived from hardwood and corn straw to adsorb Cu(II) and Zn(II) from aqueous solution. Heavy metal adsorption efficiency decreased even though total removal increased with increasing biochar concentration, suggesting that aggregation is a factor that needs to be accounted for when developing metal removal strategies using biochar. Although Cu(II) adsorption was only marginally affected by Zn(II), Cu(II) competed with Zn(II) for binding sites at Cu(II) and Zn(II) concentrations $\geqslant 1.0$ mM. The results indicated that plant-residue or agricultural waste derived biochar can act as effective surface sorbent, but that care needs to be taken when using these sorbents for the treatment of mixed waste streams.

Acknowledgements

This research was supported by Zhejiang Provincial Science and Technology Program of China (2010C33057) and by USDA/Hatch NYC-189462. Thanks to Kelly Hanley, Department of Crop and Soil Sciences, Cornell University for providing the biochars and the advices on biochar characteristic analysis.

Appendix A. Supplementary data

Supplementary data associated with this article can be found, in the online version, at doi:10.1016/j.biortech.2011.06.078.

References

Abe, I., Iwasaki, S., Iwata, Y., Kominami, H., Kera, Y., 1998. Relationship between production method and adsorption property of charcoal. TANSO 185, 277–284.

Aydin, H., Bulut, Y., Yerlikaya, C., 2008. Removal of copper(II) from aqueous solution by adsorption onto low-cost adsorbents. J. Environ. Manage. 87, 37–45.

Banat, F., Al-Asheh, S., Al-Rousan, D., 2002. A comparative study of copper and zinc ion adsorption on to activated and non-activated date-pits. Adsorpt. Sci. Technol. 20, 319–335.

Behr, J., Hellwig, P., Mantele, W., Michel, H., 1998. Redox dependent changes at the heme propionates in cytochrome c oxidase from paracoccus denitrificans: direct evidence from FTIR difference spectroscopy in combination with heme propionate^{13}C labeling. Biochemistry 37, 7400–7406.

Bhattacharyaa, A.K., Mandalb, S.N., Das, S.K., 2006. Adsorption of Zn(II) from aqueous solution by using different adsorbents. Chem. Eng. J. 123, 43–51.

Bustin, R.M., Guo, Y., 1999. Abrupt changes (jumps) in reflectance values and chemical compositions of artificial charcoals and inertinite in coals. Int. J. Coal Geol. 38, 237–260.

Cao, X.D., Harris, W., 2010. Properties of dairy-manure-derived biochar pertinent to its potential use in remediation. Bioresour. Technol. 101, 5222–5228.

Cao, X.D., Ma, L.N., Gao, B., Harris, W., 2009. Dairy-manure derived biochar effectively sorbs lead and atrazine. Environ. Sci. Technol. 43, 3285–3291.

Chen, B.L., Chen, Z.M., 2009. Sorption of naphthalene and 1-naphthol by biochars of orange peels with different pyrolytic temperatures. Chemosphere 76, 127–133.

Chen, B.L., Zhou, D.D., Zhu, L.Z., 2008. Transitional adsorption and partition of nonpolar and polar aromatic contaminants by biochars of pine needles with different pyrolytic temperatures. Environ. Sci. Technol. 42, 5137–5143.

Chun, Y., Sheng, G.Y., Chiou, C.T., Xing, B.S., 2004. Compositions and sorptive properties of crop residue-derived chars. Environ. Sci. Technol. 38, 4649–4655.

Das, D.D., Schnitzer, M.I., Monreal, C.M., Mayer, P., 2009. Chemical composition of acid-base fractions separated from biooil derived by fast pyrolysis of chicken manure. Bioresour. Technol. 100, 6524–6532.

Day, D., Evans, R.J., Lee, J.W., Reicosky, D., 2005. Economical CO_2, SO_x, and NO_x capture from fossil-fuel utilization with combined renewable hydrogen production and large-scale carbon sequestration. Energy 30, 2558–2579.

Demirbas, A., 1997. Calculation of higher heating values of biomass fuels. Fuel 76, 431–434.

Dudka, S., Adriano, D.C., 1997. Environmental impacts of metal ore mining and processing: a review. J. Environ. Qual. 26, 590–602.

El-Sofany, E.A., Zahera, W.F., Aly, H.F., 2009. Sorption potential of impregnated charcoal for removal of heavy metals from phosphoric acid. J. Hazard. Mater. 165, 623–629.

Fuertes, A.B., Camps Arbestain, M., Sevilla, M., Maciá-Agulló, J.A., Fiol, S., López, R., Smernik, R.J., Aitkenhead, W.P., Arce, F., Macias, F., 2010. Chemical and structural properties of carbonaceous products obtained by pyrolysis and hydrothermal carbonisation of corn stover. Aust. J. Soil Res. 48, 618–626.

Kuhlbusch, T.A.J., 1995. Method for determining black carbon in residues of vegetation fires. Environ. Sci. Technol. 29, 2695–2702.

Laird, D.A., 2008. The charcoal vision: a win-win-win scenario for simultaneously producing bioenergy, permanently sequestering carbon, while improving soil and water quality. Agron. J. 100, 178–181.

Lehmann, J., 2007a. A handful of carbon. Nature 447, 143–144.

Lehmann, J., 2007b. Bio-energy in the black. Front. Ecol. Environ. 5, 381–387.

Lehmann, J., Gaunt, J., Rondon, M., 2006. Bio-char sequestration in terrestrial ecosystems – a review. Mitig. Adapt. Strateg. Glob. Change 11, 403–427.

Liu, Z.G., Zhang, F.S., 2009. Removal of lead from water using biochars prepared from hydrothermal liquefaction of biomass. J. Hazard. Mater. 167, 933–939.

Martinsa, R.J.E., Pardob, R., Boaventura, R.A.R., 2004. Cadmium(II) and zinc(II) adsorption by the aquatic moss *Fontinalis antipyretica*: effect of temperature, pH and water hardness. Water Res. 38, 693–699.

Mingorance, M.D., Oliva, S.R., 2006. Heavy metals content in *N. Oleander* leaves as urban pollution assessment. Environ. Monit. Assess. 119, 57–68.

Mohan Jr, D., Pittman, C.U., Bricka, M., Smith, F., Yancey, B., Mohammad, J., Steele, P.H., Alexandre-Franco, M.F., Gomez-Serrano, V., Gong, H., 2007. Sorption of arsenic, cadmium and lead by chars produced from fast pyrolysis of wood and bark during bio-oil production. J. Colloid Interface Sci. 310, 57–73.

Monser, L., Adhoum, N., 2002. Modified activated carbon for the removal of copper, zinc, chromium and cyanide from wastewater. Sep. Purif. Technol. 26, 137–146.

Nguyen, T.H., Cho, H.H., Poster, D.L., Ball, W.P., 2007. Evidence for a pore-filling mechanism in the adsorption of aromatic hydrocarbons to a natural wood char. Environ. Sci. Technol. 41, 1212–1217.

Samonin, V.V., Nikonova, V.Yu., Podvyaznikov, M.L., 2008. The sorption properties of active carbons modified with fullerenes with respect to copper, silver and lead cations in aqueous solutions. Russ. J. Phys. Chem. A 82, 1371–1375.

Sassner, P., Galbe, M., Zacchi, G., 2008. Techno-economic evaluation of bioethanol production from three different lignocellulosic materials. Biomass Bioenerg. 32, 422–430.

Seco, A., Marzal, P., Gabaldón, C., Ferrer, J., 1997. Adsorption of heavy metals from aqueous solutions onto activated carbon in single Cu and Ni systems and in binary Cu–Ni, Cu–Cd and Cu–Zn systems. J. Chem. Technol. Biotechnol. 68, 23–30.

Shinogi, Y., Kanri, Y., 2003. Pyrolysis of plant, animal and human waste: physical and chemical characterization of the pyrolytic products. Bioresour. Technol. 90, 241–247.

Sohi, S., Lopez-Capel, E., Krull, E., Bol, R., 2009. Biochar, climate change and soil: a review to guide future research. CSIRO Land and Water Science Report 05/09, February 2009.

Spokas, K.A., Reicosky, D.C., 2009. Impacts of sixteen different biochars on soil greenhouse gas production. Ann. Environ. Sci. 3, 179–193.

Tanaka, S., 1963. Fundamental study on wood carbonization. In: Bulletin of Experimental Forest of Hokkaido University.

Uchimiya, M., Lima, I.M., Klasson, K.T., Chang, S.C., Wartelle, L.H., Rodger, J.E., 2010. Immobilization of heavy metal ions (Cu^{II}, Cd^{II}, Ni^{II}, and Pb^{II}) by broiler litter-derived biochars in water and soil. J. Agric. Food Chem. 58, 5538–5544.

Wang, H.L., Lin, K.D., Hou, Z.N., Richardson, B., Gan, J., 2010. Sorption of the herbicide terbuthylazine in two New Zealand forest soils amended with biosolids and biochars. J. Soils Sediments 10, 283–289.

Wang, X.L., Sato, T., Xing, B.S., 2006. Competitive sorption of pyrene on wood chars. Environ. Sci. Technol. 40, 3267–3272.

Wang, X.L., Xing, B.S., 2007. Sorption of organic contaminants by biopolymer-derived chars. Environ. Sci. Technol. 41, 8342–8348.

Woolf, D., 2008. Biochar as a soil amendment: a review of the environmental implications. http://orgprints.org/13268/01/Biochar_as_a_soil_amendment_-_a_review.pdf.

Yang, Y.N., Sheng, G.Y., 2003. Enhanced pesticide sorption by soils containing particulate matter from crop residue burns. Environ. Sci. Technol. 37, 3635–3639.

Yenisoy-Karakas, S., Aygun, A., Gunes, M., Tahtasakal, E., 2004. Physical and chemical characteristics of polymer-based spherical activated carbon and its ability to adsorb organics. Carbon 42, 477–484.

Yu, X.Y., Pan, L.G., Ying, G.G., Kookana, R.S., 2010. Enhanced and irreversible sorption of pesticide pyrimethanil by soil amended with biochars. J. Environ. Sci. 22, 615–620.

Zhu, D.Q., Kwon, S., Pignatello, J.J., 2005. Adsorption of single-ring organic compounds to wood charcoals prepared under different thermochemical conditions. Environ. Sci. Technol. 39, 3990–3998.